Cell

Mutations in Potassium Channel Kir2.6 Cause Susceptibility to Thyrotoxic Hypokalemic Periodic Paralysis

Devon P. Ryan,[1,2,14] Magnus R. Dias da Silva,[2,14,15] Tuck Wah Soong,[4,8] Bertrand Fontaine,[5] Matt R. Donaldson,[2,16] Annie W.C. Kung,[6] Wallaya Jongjaroenprasert,[7] Mui Cheng Liang,[8] Daphne H.C. Khoo,[10] Jin Seng Cheah,[9] Su Chin Ho,[10] Harold S. Bernstein,[11] Rui M.B. Maciel,[12] Robert H. Brown, Jr.,[13] and Louis J. Ptáček[1,2,3,*]

[1]Neuroscience Graduate Program
[2]Department of Neurology
[3]Howard Hughes Medical Institute
University of California, San Francisco, San Francisco, CA, 94158, USA
[4]Ion Channel and Transporter Laboratory, National Neuroscience Institute, Singapore 308433, Republic of Singapore
[5]INSERM, Université Pierre et Marie Curie-UPMC, UMRS 546, and Assistance Publique-Hôpitaux de Paris, Centre de Référence des Canalopathies Musculaires, Groupe Hospitalier Pitié-Salpêtrière, 75013 Paris, France
[6]Department of Medicine, University of Hong Kong, Queen Mary Hospital, Hong Kong SAR, China
[7]Department of Medicine, Ramathibodi Hospital, Mahidol University, Bangkok 10400, Thailand
[8]Department of Physiology
[9]Department of Medicine
Yong Loo Lin School of Medicine, National University of Singapore, Singapore 308433, Republic of Singapore
[10]Department of Clinical Research, Singapore General Hospital, Singapore 169608, Republic of Singapore
[11]Cardiovascular Research Institute, University of California, San Francisco, San Francisco, CA 94143-0130, USA
[12]Department of Medicine, Division of Endocrinology, Universidade Federal de São Paulo, São Paulo 04039-032, Brazil
[13]Massachusetts General Hospital, 16th Street, Navy Yard, Charlestown, MA 02129, USA
[14]These authors contributed equally to this work
[15]Present address: Department of Biochemistry, Universidade Federal de São Paulo, São Paulo 04044-020, Brazil
[16]Present address: Department of Dermatology, Texas Tech University, Lubbock, TX 79409, USA
*Correspondence: ljp@ucsf.edu
DOI 10.1016/j.cell.2009.12.024

SUMMARY

Thyrotoxic hypokalemic periodic paralysis (TPP) is characterized by acute attacks of weakness, hypokalemia, and thyrotoxicosis of various etiologies. These transient attacks resemble those of patients with familial hypokalemic periodic paralysis (hypoKPP) and resolve with treatment of the underlying hyperthyroidism. Because of the phenotypic similarity of these conditions, we hypothesized that TPP might also be a channelopathy. While sequencing candidate genes, we identified a previously unreported gene (not present in human sequence databases) that encodes an inwardly rectifying potassium (Kir) channel, Kir2.6. This channel, nearly identical to Kir2.2, is expressed in skeletal muscle and is transcriptionally regulated by thyroid hormone. Expression of Kir2.6 in mammalian cells revealed normal Kir currents in whole-cell and single-channel recordings. Kir2.6 mutations were present in up to 33% of the unrelated TPP patients in our collection. Some of these mutations clearly alter a variety of Kir2.6 properties, all altering muscle membrane excitability leading to paralysis.

INTRODUCTION

The periodic paralyses and nondystrophic myotonias comprise a group of muscle disorders characterized by abnormal muscle relaxation (myotonia) and/or paroxysmal muscle weakness. These disorders are subdivided on the basis of the presence of myotonia with weakness, response to potassium, temperature sensitivity, association with cardiac arrhythmia and facial dysmorphology, and induction by thyrotoxicosis. Many of these entities are now known to result from ion channel mutations, termed channelopathies (Ryan and Ptácek, 2007).

TPP is a sporadic muscle disorder characterized by episodic attacks of weakness and hypokalemia in some thyrotoxic individuals. Patients are normal between attacks, which resolve with treatment of thyrotoxicosis. Episodic weakness in TPP is clinically similar to the known channelopathies familial hypoKPP and Andersen-Tawil syndrome (ATS) (Bulman et al., 1999; Plaster et al., 2001; Ptácek et al., 1994) and is the most common form of periodic paralysis, being most prevalent in young Asian and Latin American men (Kung, 2006; Silva et al., 2004). In these populations, up to 10% of thyrotoxic male individuals develop

episodic weakness. In Caucasians, this number is less than 0.1% (Kelley et al., 1989). Although thyrotoxicosis is more common in women, most individuals with TPP are men.

Aside from similarity to the familial periodic paralyses, several observations indicate that TPP may be a genetically conditioned disorder unmasked by thyrotoxicosis. Although weakness is a common symptom of thyrotoxicosis, episodic flaccid paralysis arises in only some thyrotoxic patients. TPP recurs in patients with recurring hyperthyroidism, such as relapses of Graves Disease (Kung, 2002), and, as with other channelopathies, a similar phenotype is seen across species (Nemzek et al., 1994).

While screening skeletal muscle ion channel candidate genes in TPP patients, we serendipitously identified a previously unreported gene—here named *KCNJ18*—encoding an inwardly rectifying potassium channel, Kir2.6. This subfamily, which includes Kir2.1 through Kir2.4 and Kir2.2v/Kir2.5, is one of seven subfamilies (Kir1.x to Kir7.x). Kir subunits have two membrane-spanning domains, are selective for potassium, stabilize the resting membrane potential near the potassium equilibrium potential, and tetramerize to form functional, inwardly rectifying channels (Krapivinsky et al., 1998; Nichols and Lopatin, 1997).

The structural and functional homology of these channels suggests they arose through gene duplication with subsequent diversification. This process plays a crucial role in evolution, allowing redundant gene variants to acquire novel characteristics and functions, with a likely role in expanding protein diversity. Kir channels have assumed specific functions in excitable tissues and mutations in these channels can cause human disease. Kir channelopathies include the episodic muscle and developmental features of ATS (Kir2.1), the renal tubular secretion defects seen with Barter syndrome type III (Kir1.1), and defective insulin secretion in persistent hyperinsulinemic hyperglycemia of infancy (Kir6.2) (Abraham et al., 1999; Plaster et al., 2001).

Kir2.6 shares 99% identity with Kir2.2 and was considered an excellent candidate for TPP because it is primarily expressed in skeletal muscle and probably contributes to cell membrane excitability. Furthermore, *KCNJ18* has a thyroid hormone response *cis* element (TRE) within its promoter, which might drive increased expression of Kir2.6 to protect against membrane potential instability.

Genetic analysis revealed mutations in Kir2.6 in multiple TPP patients. Electrophysiological analysis indicates that some of these mutations have large effects on Kir2.6 currents either inherently or via thyroid hormone-inducible mechanisms. As such, mutations may cause predisposition for the episodic weakness seen only during thyrotoxicosis.

RESULTS

Screening Candidate Genes and Genomic Characterization of *KCNJ18*

Since ion channel mutations cause familial periodic paralysis, we screened ion channels known to be expressed in skeletal muscle with putative thyroid response elements (TREs) of the DR-4 motif in their promoter regions, for mutations (Table S1 available online). While screening *KCNJ12*, we noted a number of polymorphisms that violated Hardy-Weinberg equilibrium, suggesting the existence of another gene. By changing PCR methods and primers, we specifically amplified a highly homologous sequence that we have submitted under NCBI accession number FJ434338 as *KCNJ18*.

Sequencing of ten clones from low-stringency PCR yielded the known genes *KCNJ12* (Kir2.2) and *KCNJN1/KCNJ17* (Kir2.2v/Kir2.5). In addition, a previously unreported paralog *KCNJ18* (Kir2.6, Figure 1) was seen, which shares 98%–99% identity in the coding region (96%–99% at the amino acid level, depending on the SNPs present in *KCNJ18*) with *KCNJ12* (Tables S2 and S3), shares >95% identity with *KCNJ17* (data not shown), and is only one amino acid different from *KCNJ12X* (AB181299).

To verify that *KCNJ18* is a paralogous locus, a human bacterial artificial chromosome (BAC) DNA library was screened for *KCNJ18* and *KCNJ12* by PCR with gene-specific primers. Two nonoverlapping BAC clones contained either *KCNJ18* (RP11-437N10) or *KCNJ12* (RP11-728e14). A Southern blot performed on BamHI-digested RP11-437N10 yielded a 2.6 Kb fragment (Figure 2B). Furthermore, we are unable to specifically amplify *KCNJ12* from RP11-437N10, but are able to do so from RP11-728e14, as confirmed by sequencing of the PCR product. The reverse is true for specific amplification of *KCNJ18* (Figure 2C). It appears that during the analysis and alignment of genome sequences, the high identity between *KCNJ12* and *KCNJ18* resulted in nonhomologous end joining of nonoverlapping BACs and, therefore, exclusion of *KCNJ18*. Based on sequencing of both ends of RP11-437N10, we locate this BAC centromeric to *KCNJ12* in the same chromosomal segment, where there is currently a gap (Figure 2D). Taken together, these data suggest that the two homologs arose through duplication of this region (Figure S2).

The flanking 5′ and 3′ untranslated regions (UTRs) of *KCNJ12* and *KCNJ18* were characterized by rapid amplification of cDNA ends (RACE), using the unique nucleotides at the 3′ end of the primers from the coding sequence as the gene-specific primers. Despite the high homology, unique upstream sequences were noted in RACE clones in the 5′ UTR. Sequencing of the BACs revealed a unique exon 1 for each gene. We obtained the Kir2.6 cDNA from a human testis cDNA pool using specific outer primers designed from the RACE clone sequences. The forward primer was taken from the unique exon 1 sequence and the reverse from the 3′ UTR. Each of the DNA sequence variants found in the *KCNJ18* BAC clone that differ from *KCNJ12* are also present in the full-length *KCNJ18* cDNA, establishing it as an independent transcript. This transcript was also amplified from pooled human brain and skeletal muscle cDNA. For both genes, exon 3 contains the entire coding region, (Figure 1A).

Probes for the unique exon 1 of *KCNJ12* and *KCNJ18* were used for northern blot analysis. Both transcripts are highly expressed in skeletal muscle (Figures 3A–3C) and the transcript sizes differ (~2.2 Kb for *KCNJ12*, ~6 Kb for *KCNJ18*).

Triiodothyronine Enhances *KCNJ18* Transcription

We tested whether *KCNJ18* transcription is regulated by triiodothyronine (T3) since there is a putative TRE (in reverse strand) between nucleotides −265 and −249 (5′-TGACCTGGCCTcACC TCAGGG-3′), which differs from the consensus TRE by only 1

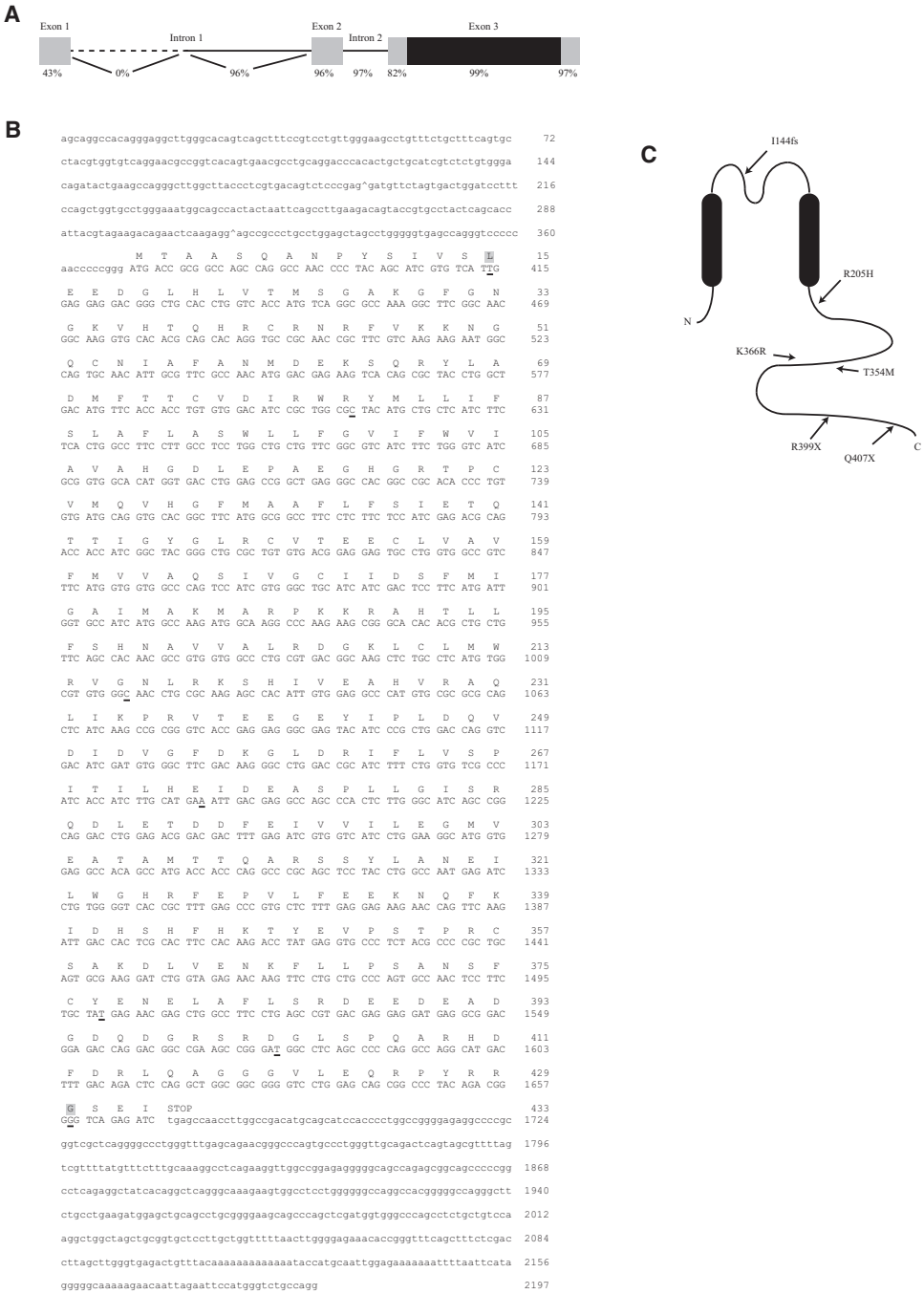

Figure 1. Structure and Sequence of *KCNJ18* and Kir2.6

(A) *KCNJ18* shares a high degree of identity with *KCNJ12* in both exons (boxes) and introns (lines). The coding region of both *KCNJ18* and *KCNJ12* is contained within exon 3 (black region). The first intron of *KCNJ12* is longer than that of *KCNJ18*, causing 0% identity in this nonoverlapping region (dotted line).

(B) *KCNJ18* sequence-exon boundaries are denoted with a caret (^). Coding sequence is capitalized with the corresponding amino acid above. Underlined nucleotides denote differences between *KCNJ18* and *KCNJ12*, with nonsynonymous differences having a gray background.

(C) Diagram of Kir2.6 with the relative locations of TPP associated mutations.

See also Figure S1.

base pair (c). This is a direct motif repeat with a 4 nt link (DR4). A luciferase assay in mammalian cells overexpressing thyroid hormone (TR) and retinoid X receptor (RXR) was used to determine whether this TRE motif is functional. Mouse skeletal muscle myoblasts (C2C12) or human embryonic kidney cells (293T) were transfected with reporter constructs containing the

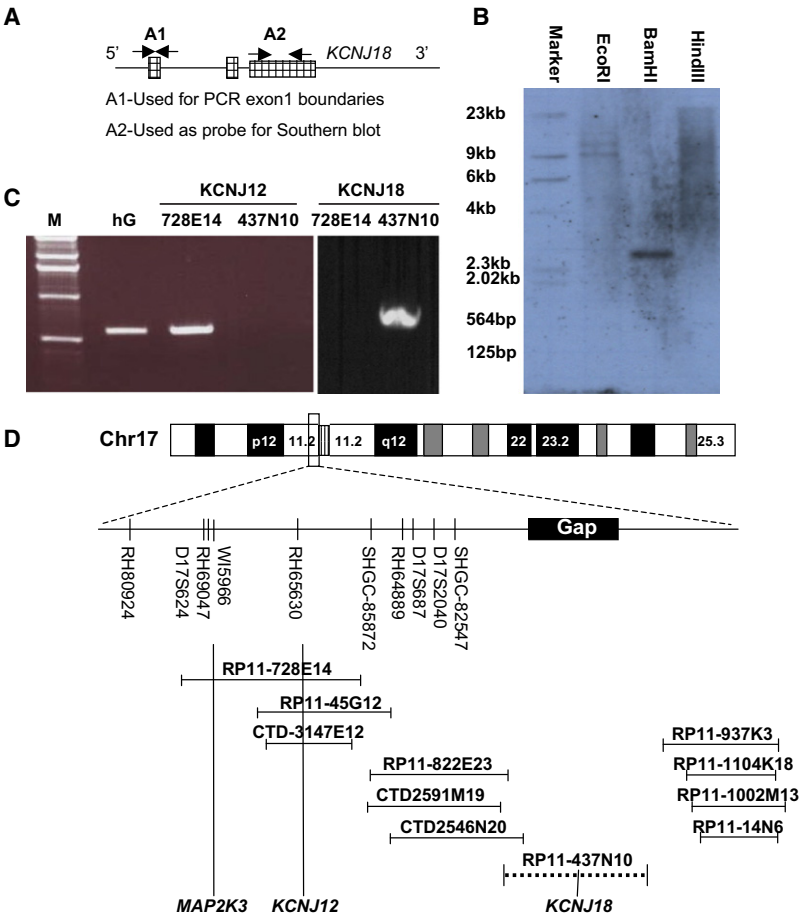

Figure 2. Genomic Characterization of *KCNJ18*

(A) Both *KCNJ12* and *KCNJ18* have three recognized exons (hatched regions). Probes constructed from exon 1 (A1, unique for each gene) were used for northern blot and genome walking to determine exon 1 boundaries.

(B) Radiolabeled A2 primers from exon 3 were used as a probe for Southern blot upon BamH1-digested *KCNJ18* containing BAC DNA,

(C) *KCNJ12* specific primers were able to yield PCR products from control human genomic (hG) DNA and BAC RP11-728E14 (containing *KCNJ12*) but not RP11-437N10 (containing *KCNJ18*).

(D) From this BAC end sequencing, we place *KCNJ18* centromeric to *KCNJ12* on chromosome 17 in a previously identified sequencing gap and not overlapping with *KCNJ12*.

See also Figure S2.

KCNJ18/TRE-pGL3 wild-type (WT), negative controls consisting of mutant (Mut) or empty pGL3 vector (Emp), and positive control (2xDR4-pGL3). The WT construct produced high luciferase activity compared to controls and responded in a dose-dependent fashion to T3. However, the truncated Mut construct produced only 25% and 7% as much luciferase activity as WT in 293T and C2C12 cells, respectively (Figure 3D). These results corroborate our data from an electrophoretic mobility shift assay with nuclear extracts from a pool of TR-transfected 293T cells (data not shown).

Mutational Analysis of *KCNJ18* in TPP Patients

The *KCNJ18* coding region was specifically amplified and sequenced in 30 TPP patients collected from the United States, Brazil, and France. Five mutations were found. Two C-to-T transitions, c.C1195T (R399X) and c.C1219T (Q407X), were identified in one and five affected individuals, respectively. Missense mutations c.C1061T (T354M) and c.A1097G (K366R) were identified in a single patient each. Two further patients, both from France, presented with both a T140M mutation and a single nucleotide deletion (c.428 delC) leading to a frameshift with a stop codon at position 151 (I144fs). The T140M mutation appears alongside the I144fs mutation, which is the likely causative change. These mutated residues are well conserved in Kir2 channels (Figure S1). None were found in 281 healthy controls

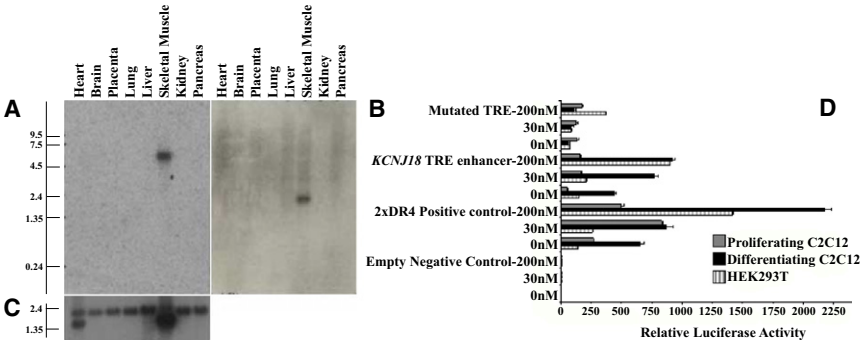

Figure 3. Expression Pattern and Transcriptional Regulation of *KCNJ18*

(A and B) The A1 probe set (Figure 2A) was used to specifically probe multiple tissue northern blot membranes for *KCNJ18* (A) and *KCNJ12* (B) mRNAs, which are found specifically in skeletal muscle.

(C) β-actin was used as a loading control.

(D) The *KCNJ18* regulatory region can function as an enhancer for luciferase expression in HEK293T and either proliferating or differentiated C2C12 cells. A DR4-positive control, an empty vector control, and a mutated *KCNJ18* TRE control were also tested. Luciferase expression by the WT *KCNJ18* is enhanced in a T3 dose-dependent manner from 0 nM T3 (hypothyroid) through 200 nM (hyperthyroid) T3 after compensating for the internal renilla control. Error bars indicate the mean ± standard error.

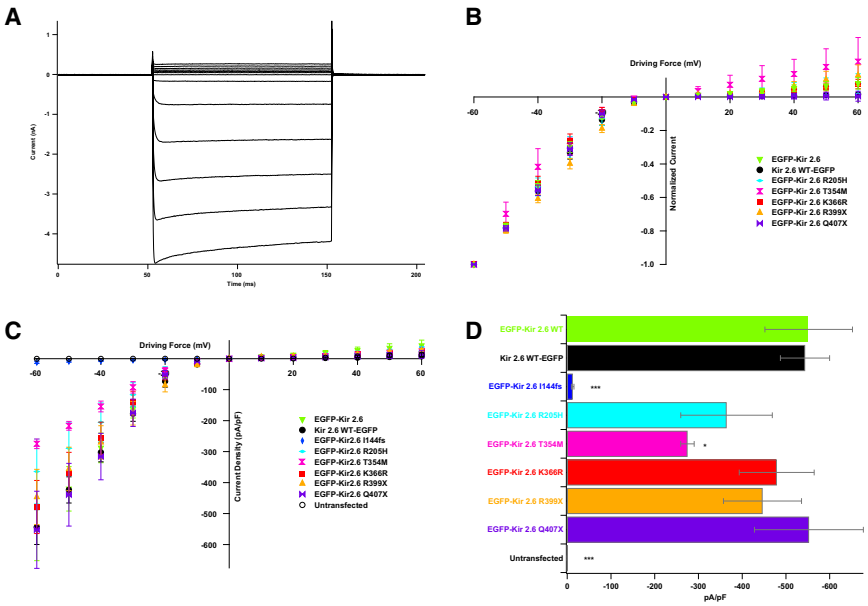

Figure 4. *KCNJ18* Encodes an Inwardly Rectifying Potassium Channel Whose Conductance Properties Are Altered by Some TPP Mutations

(A) When expressed in 293T cells, Kir2.6 produces stereotypical Kir currents. Voltage steps were performed from the resting membrane potential (0 mV driving force) to between −60 and +60 mV in increments of 10 mV.

(B) Normalization of these values to maximal current allows for comparison of rectification between WT and mutant channels. TPP mutations do not lead to altered rectification.

(C) Current density can instead be measured by normalizing currents to cellular capacitance.

(D) Both the I144fs and T354M mutations lead to decreased current density, most easily seen at −60 mV. p values were calculated with a t test versus EGFP-Kir2.6 WT. There are five to 12 cells per data point. Error bars indicate the mean ± standard error.

See also Figure S3.

(137 Caucasians, 48 Mexicans, 45 African Americans, 43 Chinese, and eight Japanese-Brazilians). Since TPP is highly prevalent in Asian thyrotoxic patients, we sequenced *KCNJ18* in TPP patients from Hong Kong, Thailand, and Singapore. One of 83 TPP subjects from Hong Kong harbored a mutation (R205H), none of 31 Thai subjects harbored mutations, and seven of 27 Singaporean subjects harbored mutations (all R399X). R399X was found in one of 76 Singaporean control samples, as expected from the prevalence of TPP among thyrotoxic individuals. No mutations were found in 98 Hong Kong thyrotoxic controls not manifesting TPP. Results are summarized in Table S4, and the mutation positions within Kir2.6 are indicated in Figure 1C.

Electrophysiology of WT and Mutant Kir2.6

Kir2.6 channels were fused to EGFP (N-terminal for the mutant and both C-terminal and N-terminal for the WT) and expressed in 293T cells. Whole-cell recordings of WT-expressing cells indicate that Kir2.6 produces typical inwardly rectifying currents (Figure 4A). This inward rectification is vital for the proper function of skeletal muscle as it allows potassium current around the resting membrane potential but not during action potentials. Normalization of currents to that produced at −60 mV allows comparison of rectification, which is unaffected by any of the TPP mutations (Figure 4B). Some of the mutations alter current density (Figures 4C and 4D). The I144fs mutation results in a complete loss of current while the T354M mutation causes a small decrease in current density. Cotransfection of the I144fs mutation with WT channels (fused to the C terminus of EYFP) indicates that I144fs does not exert a dominant negative effect (Figure S3).

Kir2.2 has a single-channel conductance of 30–34 pS and a high open probability (P_o) (Preisig-Müller et al., 2002; Takahashi et al., 1994). Kir2.6 has identical single-channel characteristics, with a conductance of approximately 34 pS and a P_o of ~80% (Figures 5A–5C).

PKC activation, which is increased during thyrotoxicosis, results in decreased Kir2.2 whole-cell currents, and threonine 354 is involved in this process (Karle et al., 2002). As the equivalent Kir2.6 residue is mutated in one TPP patient, we tested whether phosphorylation of this residue alters single-channel characteristics and whether the T354M mutation abrogates these alterations. The single-channel conductance and P_o of the T354M mutant are identical to WT Kir2.6 channels (Figures 5B and 5C). Activation of PKC with phorbol 12-myristate 13-acetate (PMA) does not seem to alter the single-channel conductance of either the mutant T354M (35.7 ± 0.85 pS with PMA versus 33.8 ± 0.89 pS without) or WT channels (32.8 ± 3.0 pS with PMA versus 34.2 ± 0.9 pS without, Figure 5B). However, while PKC activation does not alter the P_o of mutant channels, it nearly abolishes that of WT channels (WT, 78.9% ± 0.9%; WT + PMA, 0.00069% ± 0.00033%; T354M, 82.1% ± 0.8%; T354M + PMA, 84.2% ± 0.8% average across voltages, Figure 5C). Similarly, mimicking pseudoconstitutive phosphorylation of this residue (T354E) results in unaltered single-channel conductance (30.5 ± 0.17 pS) and a decreased P_o (0.00093% ± 0.00048%).

Kir channel interactions with phosphatidylinositol-(4,5) bisphosphate (PIP_2) occur via positively charged residues in the C termini and are required for the opening of mammalian Kir channels. Mutation of such residues in Kir2.1 leads to ATS (Donaldson et al., 2003). PIP_2 turnover is increased during thyrotoxicosis, and we hypothesized that the R205H and K366R mutations may alter interactions with PIP_2 (Kavok et al., 2001). We artificially decreased the availability of membrane PIP_2 with polylysine and measured the time for channel openings to decrease, as measured by the T_{50} time constant. Both the R205H and K366R mutations cause an ~1.5-fold increase in T_{50}, (WT, T_{50} 38.98 ± 0.016 s, base 0.85 ± 5.08e-4, A 7.82 ± 1.68e-3; R205H, T_{50} 55.34 ± 0.016 s, base 0 ± 3.78e−4, A 6.0 ± 7.88e−4; K366R, T_{50} 58.47 ± 0.024 s, base 1.02 ± 8.13e-4, A 8.92 ± 1.56e-3; Figures 6A–6D, $p < 0.001$

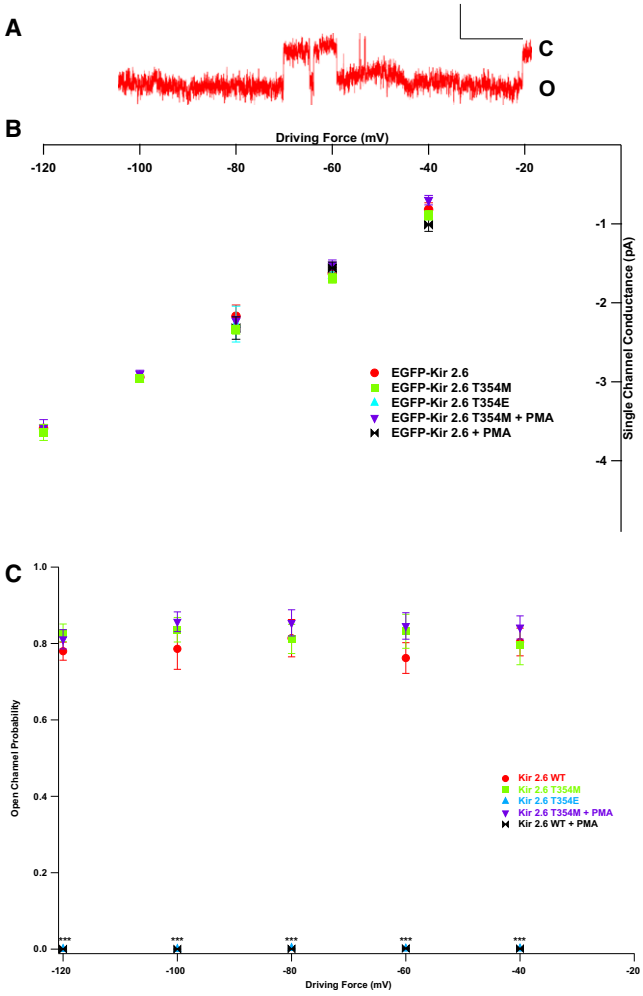

Figure 5. TPP Mutations in Kir2.6 Alter Single-Channel Response to PKC

(A) Kir2.6 produces stereotypical single-channel currents. Scale bars represent 200 ms by 2 pA. Openings (O) are down, and closings (C) are up.

(B) Wild-type and mutant single-channel conductance is unaltered by PKC activation or mimicking constitutive phosphorylation at T354 (T354E).

(C) Open probability, however, is decreased in WT but not T354M mutant channels by the activation of PKC or T354E. p values were calculated a t test versus EGFP-Kir2.6 WT. There are five to nine patches per data point, each with one to three (typically two or three) channels.

according to Figure S4). This increase in T_{50} indicates that mutant channels may produce more current than WT channels during thyrotoxicosis when PIP_2 turnover is increased.

DISCUSSION

Genomic Context of *KCNJ18*

We have identified *KCNJ18* as a paralog of *KCNJ12* sharing up to 99% identity in coding sequence and having largely similar UTR and intron sequences. Because of this remarkable similarity, amplification of *KCNJ12* for sequencing inadvertently amplified *KCNJ18*; sequence differences were previously interpreted as heterozygosity for polymorphic alleles for a single gene (*KCNJ12*), though we now present evidence for two unique genes. Duplicated regions are enriched in or around sequence gaps, such as that containing *KCNJ18*, and are known to be difficult to recognize (Bailey et al., 2001; Eichler et al., 2004). It has been estimated that over 5% of the human genome is composed of duplicons, large regions (1 to over 100 Kb) of duplicated sequence sharing high (>90%) identity (Bailey et al., 2001). Such regions are thought to result from inter- or intrachromosomal segmental duplication, with the latter involving DNA flanking pericentromeric regions.

KCNJ18 is not the first paralog of *KCNJ12* to be reported. *KCNJ17* (Kir2.5) has 95% identity to *KCNJ12*, but the GYG selectivity filter is changed to SYG, rendering it nonfunctional (Namba et al., 1996). We verified that *KCNJ17* is a third paralog using gene-specific primers to amplify it from control and patient DNA along with *KCNJ12* and *KCNJ18*.

The exact positions of *KCNJ18* and *KCNJ17* remain unclear. Although a BAC containing *KCNJ17* has not been found, both RP11-437N10 (containing *KCNJ18*) and RP11-728e14 (containing *KCNJ12*) have been mapped to 17p11.1-2. *KCNJ12* and *KCNJ17* were originally localized to 17p11.1 by FISH (Hugnot et al., 1997; Namba et al., 1997). According to the BAC sequences, we localize *KCNJ12* and *KCNJ18* to this pericentromeric region. Although pericentromeric duplications are thought to contain heterochromatic DNA and have fewer expressed genes, we have presented several lines of evidence suggesting that *KCNJ18* is transcribed and functional and that the BAC containing it is distinct.

Regulation of Kir2.6 Expression

Protein regulation by thyroid hormones is complex, occurring both by transcriptional and posttranslational events (Bassett et al., 2003). Transcriptional regulation is particularly important in skeletal muscle, where both decreased (hypothyroidism) and increased (thyrotoxicosis) T3 has a profound effect on muscle performance. Some channels, such as Kv1.5 and Kv4.2, are known to be transcriptionally regulated by T3, while T3 regulation of Kir transcription has received little attention (Le Bouter et al., 2003). To determine the feasibility of T3 altered transcription, we searched for putative thyroid response elements (TREs) in the regulatory region of these genes using the publicly available TESS-TRANSFAC v6.0 software (http://www.cbil.upenn.edu/tess/). Based on 2 Kb of sequence 5′ upstream of *KCNJ18*, we identified four putative TREs with Lq scores of 0.9 to 1 (the best is 1), with a mismatch allowance of 10%. Of these, only a single predicted TRE of the DR4 variety had a high score. A similar search of the regulatory region of *KCNJ12* identified no putative TREs.

To add credence to these predictions, we found that TRβ-T3 complexes bind to these TRE-*KCNJ18* sequences. Luciferase assay results show that the regulatory region of *KCNJ18* confers dose-dependent T3 transcriptional modulation (Figure 3) in HEK293 and differentiated C2C12 cells.

Possible Role of Kir2.6

Multiple-tissue northern blotting revealed a skeletal muscle-specific pattern of both Kir2.2 and Kir2.6 expression. To prevent

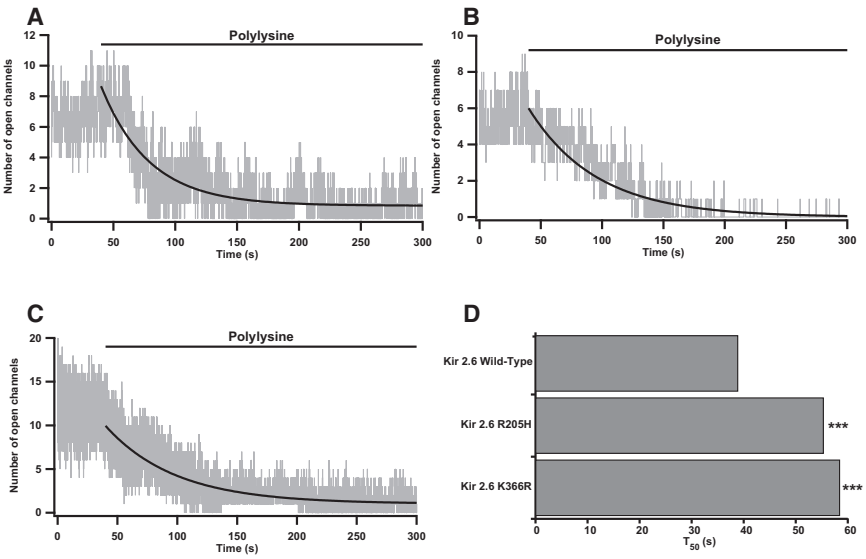

Figure 6. Kir2.6-PIP_2 Interactions Are Altered by TPP Mutations

(A–C) Inside-out patches were perfused with isotonic solution for 40 s prior to perfusion with polylysine. Wild-type (A), R205H (B), and K366R (C) openings decreased after polylysine perfusion.

(D) Curve fits of idealized channel openings (smooth black curves in A–C), were used to derive the T_{50} value. Both the R205H and the K366R mutant channels have an altered interaction with PIP_2 and take significantly longer to reach half-maximal opening than WT channels. There are five to ten cells and nine to 20 total channels per channel type. $p < 0.001$ in accordance to a statistical model.

See also Figure S4.

nonspecific detection of similar transcripts, we performed these blots by probing against the unique exon 1. Earlier expression studies in human (heart only) and mouse (multiple tissues) suggest that Kir2.2 is expressed abundantly in many tissues, including heart, skeletal muscle, and neurons (Takahashi et al., 1994; Wible et al., 1995). However, the probes used in these experiments were designed against the coding region of Kir2.2 (exon 3), which shares high identity with the other members of the Kir2 family. Thus, it is likely that probes used in previous reports were nonspecific for Kir2.2. These blots using human atrium and multiple mouse tissues revealed bands of multiple sizes. As shown in Figure 2, our probes detected single transcripts of 6 and 2.2 Kb. This difference in transcript size between *KCNJ12* and *KCNJ18*, as well as nonspecific detection of other Kir channels, may explain the previously observed pattern that has been interpreted as variable UTR extension. Sequences identified through RACE are shorter than bands of 6 and 2.2Kb detected on northern blot. Thus, there may be additional, unrecognized noncoding exons.

Kir2.6 shares 96%–99% amino acid identity with Kir2.2 (depending on the SNPs present) and high homology of introns (>95%). Kir2.2 is a member of the strong inward rectifier subfamily (Preisig-Müller et al., 2002; Takahashi et al., 1994). It is thought that Kir2s maintain the resting membrane potential in excitable cells (Takahashi et al., 1994; Wible et al., 1995). Kir2.1 and Kir2.2 share over 70% identity at the amino acid level, overlap in expression, and may coassemble, leading to the repolarization of I_{K1} current in mouse heart (Preisig-Müller et al., 2002; Zaritsky et al., 2000; Zaritsky et al., 2001; Zobel et al., 2003). While the role of Kir2 channels in skeletal muscle has received much less attention, it appears largely similar to that in cardiac myocytes. Increased or decreased ion channel transcription during thyrotoxicosis may cause drastic changes in resting membrane potential and potassium accumulation and can lead to weakness in otherwise normal patients. We propose that Kir2.6 levels are increased during thyrotoxicosis to aid in proper membrane potential maintenance, warding off more severe weakness.

Mutations in Kir2.6 Cause Susceptibility to TPP

We have found a total of six mutations in Kir2.6 associated with TPP. These mutations are largely localized in the channel's intracellular C terminus with a single frame-shift truncation mutation in the pore region. These mutations account for up to 33% of patients in the United States/Brazil/France group, indicating that other TPP genes exist. Kir2.6 mutations were identified in ~25% of Singaporean patients (seven of 27) but in only one of 83 patients from Hong Kong and 0 of 31 Thai patients. Thus, there are unique genetic contributions to TPP in different ethnic populations. Genetic complexity is not surprising given the complex affect of thyroid hormones on both transcription and posttranslational modification. These differences in mutation frequency between Asian populations are likely due to genetic heterogeneity between and (as for the Chinese population) within Asian populations.

Inward rectification is one of the most important properties of Kir channels, allowing for asymmetrically large current at hyperpolarized potentials. Rectification is caused by a voltage-dependent conduction-pore blockage by intracellular polyamines and Mg^{2+} (Lu, 2004). A potential gradient across the cell membrane removes this blockage during hyperpolarization but allow these polyvalent cations to occlude the ion-conducting pore during depolarizations. Rectification is important for setting the resting potential and aiding in repolarization of cells while not shunting current during depolarizations. We showed that none of the TPP mutations alter Kir2.6 rectification (Figure 4B).

The I144fs mutation results in a stop codon in the pore region and completely nonfunctional channels (Figures 4C and 4D). Truncated subunits lack the entire C terminus and M2 membrane-spanning helix. The M2 helix lines a portion of the ion-conducting pore and is involved in intersubunit coupling. The C terminus is involved in both gating and intersubunit assembly (Soom et al., 2001; Tinker et al., 1996). Coexpression studies showed that the I144fs mutation does not coassemble with WT subunits (Figure S3), presumably leading to the TPP phenotype through haploinsufficiency (Figure 7).

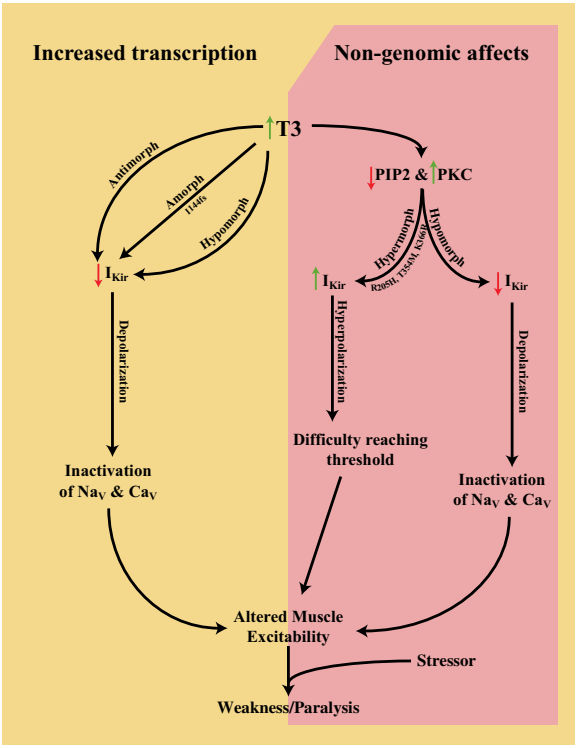

Figure 7. Model of TPP Pathophysiology

Amorphic and antimorphic alleles would cause decreased K^+ currents leading to depolarization and gradual transitioning of voltage-gated channels to their inactivated states. Hypermorphic alleles, causing hyperpolarization, conversely, would cause difficulty reaching threshold. These opposite shifts in membrane excitability, when coupled with a stressor event, are both predicted to lead to the weakness and paralysis observed in TPP. How the genomic and nongenomic effects of thyrotoxicosis on other ion channels interact with these proposed Kir current alterations remains to be elucidated.

The T354M mutation also leads to a small decrease in overall whole-cell current (Figure 4C) that is attributable to alterations of neither conductance nor open channel probability (Figures 5C and 5D). Whether this small change is physiologically relevant is unclear. We found that Kir2.6 single-channel conductance is unaltered by PKC activation while P_o is decreased dramatically in WT but not T354M channels (Figures 5B and 5C). The T354E mutation has properties identical to WT channels in the presence of activated PKC, indicating that phosphorylation of T354 causes current decrease by changing open probability. These data demonstrate that PKC activation leads to closure of WT channels but not T354M mutant channels. Such changes in PKC activity are expected during thyrotoxicosis and may result in weakness in the presence of the T354M hypermorphic mutation (Figure 7).

PKC is activated during thyrotoxicosis because of increased PIP_2 turnover (Kavok et al., 2001; Lin et al., 1999). Kir channels interact directly with PIP_2 in the membrane during normal gating, suggesting that currents are decreased during thyrotoxicosis by a decreased ability to open. This protein-lipid interaction occurs at a number of positively charged residues in the C terminus. In ATS, a number of these residues are mutated and result in decreased PIP_2 affinity (Lopes et al., 2002). Two TPP mutations, R205H and K366R, occur in positively charged residues in the C terminus and may alter PIP_2 affinity. Inside-out patches containing mutant or WT channels were perfused with polylysine to screen membrane charges and disrupt protein-lipid interactions (Lopes et al., 2002). We found that the time required for half-maximal current degradation for both of the mutants is significantly longer than that of WT channels (Figure 6D), suggesting that these are hypermorphic mutations (Figure 7).

The disease causing affects of two TPP-associated mutations (R399X and Q407X) have not yet been fully elucidated. Both of these mutations are located at the very C terminus of the channel and result in the absence of a putative PDZ interacting domain important for proper subcellular localization of Kir2.2 in skeletal muscle (Leonoudakis et al., 2004a, 2004b). We found that these mutant channels are functional in 293T cells and localize to the membrane in both these and C2C12 cells. However, mutant channels may either have improper trafficking or localization in native skeletal muscle. Such changes likely result in decreased or misplaced Kir2.6 currents, possibly in a dominant negative fashion. Ongoing experiments are aimed at addressing these questions.

We present a previously unreported paralog of Kir2.2 that encodes a strong inwardly rectifying potassium channel, Kir2.6, sharing up to 99% amino acid identity. As mutations in other ion channels are known to cause familial periodic paralysis, we screened this and other ion channels for mutations. We present genetic and electrophysiological evidence that mutations in Kir2.6 underlie TPP in a significant portion of patients. These mutations probably lead to paralysis only during thyrotoxicosis because Kir2.6 levels are increased by these conditions, nongenomic effects of T3 alter posttranslational modifications, and muscle membrane potential is already metabolically stressed by changes in many other ionic currents. Further functional characterization will determine the affects of the remainder of TPP associated mutations and whether mutant channels can coassemble with other WT Kir subunits with physiologically relevant effects. Homologs of ion channel genes identified as the cause of familial periodic paralysis were later shown to cause cardiac arrhythmias including long-QT syndrome. It is therefore interesting to speculate that the atrial fibrillation frequently seen in thyrotoxic patients may be due, in part, to both genomic and nongenomic affects of thyroid hormones on inward rectifiers and other channels expressed in the heart.

EXPERIMENTAL PROCEDURES

Identification of Patients with TPP

We collected DNA and clinical data on unrelated index patients. TPP was diagnosed in patients with episodic flaccid paralysis, hypokalemia during at least one of the attacks, and altered thyroid function tests. Written consent was obtained from all subjects in compliance with the Institutional Review Boards and Ethics committees at the University of California at San Francisco, the Federal University of Sao Paulo, the University of Hong Kong, Groupe Hospitalier-Pitié-Salpêtrière, Ramathibodi Hospital, Singapore General Hospital, National University Hospital (Singapore), and the National Neuroscience Institute (Singapore). Ethnicity of both patients and controls was determined by self-report.

We confirmed the diagnosis of thyrotoxicosis through the findings of suppressed TSH and elevated free T4 and/or total T3, measured by an

immunofluorimetric method (Delphia-Wallac, Finland); TSH-receptor antibodies (TRAb) by a radioassay (BRAHMS, Germany); and anti-thyroid peroxidase and anti-thyroglobulin antibodies by radioimmunoassays (BRAHMS, Germany). Potassium was measured via ion-specific electrode (normal is between 3.5 and 5.0 mmol/l). Clinical results from select patients are summarized in Table S5.

Low-Stringency PCR

Genomic DNA was extracted from leucocytes with PUREGENE DNA isolation blood kits (GENTRA Systems, Minneapolis, MN). PCR primers were designed against the GenBank accession NM_021012 sequence with the forward primer containing two nucleotide mismatches to favor amplification of diverse products. In brief, a standard outer PCR reaction (primers: TGGTGTC GTCTCTGTTCC/CTGGGCCCGTTCTGCTC) was performed employment of 100–200 ng genomic DNA in 50 μl containing 90% Platinum PCR SuperMix (Invitrogen, Carlsbad, CA). Cycling conditions were as follows: 5 min at 94°C followed by 38 cycles of 20 s at 94°C, a low-stringency annealing step of 30 s at 56°C, and an extension step of 2 min at 72°C.

We performed nested PCR of Kir2.2 with 20 ng outer PCR product in 50 μl containing 10 mM Tris-HCl (pH 9 at 25°C), 50 mM KCl, 0.1% Triton X-100, 200 μM each dNTP, 1.5 mM MgCl2, 1 U Taq DNA polymerase, and 25 pmol forward and reverse primers (CGAGGAGGGCGAGTACATC/CAAGATGGT GATGGGCG) under the following conditions: five cycles at 66°C for 30 s and 72°C for 1 min, plus 30 cycles at 64°C for 30 s and 72°C for 1 min, each cycle preceded by a 94°C step. The resulting products were subcloned into pCR2.1 (Invitrogen, Carlsbad, CA) and sequenced.

BAC Southern Blot

Five micrograms of purified BAC DNA was digested with EcoRI and BamHI (New England Biolabs, Beverly, MA) for 16 hr and then fractionated on a 1% agarose gel before blotting to a Nylon membrane (Roche, Indianapolis, IN) by capillary transfer. *KCNJ12* PCR product was released from pCR2.1 by EcoRI digestion, gel purified, and random prime performed at 37°C with the Digoxigenin-labeled system (DIG Luminescent Detection Kit, Roche). Hybridization was performed at 68°C overnight in hybridization buffer (6× SSC, 5× Denhardt's reagent, 0.5% SDS, and 100 μg/mL salmon sperm DNA). The membrane was washed 2 × 20 min in 2× SSC/0.1% SDS at room temperature followed by 2 × 20 min washes in SSC/0.1% SDS at 65°C. The membrane was then exposed for 40 min with Lumi-Film Chemiluminescent Detection film (Roche Applied Science) with an intensifying screen. The gel band that matched with the blot band was cut, purified, and subcloned into pBluescript SK(+). This clone contained a 2.6 Kb BAC DNA fragment containing *KCNJ18*.

For the supplemental figures, 20 μg BAC DNA was digested with either BamHI or HindIII and fractionated on a 0.8% agarose gel prior to transfer to an Amersham Hybond-N+ membrane (GE Healthcare) and probed as above. Overnight hybridization was performed at 40°C with biotinylated oligonucleotide per the manufacturer's instructions (North2South Chemiluminescent Hybridization and Detection Kit, Pierce). Exon 1 probes are CTGTTGGGAA GCCTGTTTC and GTCACGAGGGTAAGCCAAGC. Exon 3 probes are CAACCCCTACAGCATCGTGTC and TCCACACAGGTGGTGAACAT.

Characterization of the 5′ and 3′ UTRs of *KCNJ18*

Based on the differences between *KCNJ12* (NCBI database) and *KCNJ18* (2.6 Kb clone), we performed 5′ and 3′ RACE to characterize both transcripts and their exon-intron genomic structure. The first round of RACE-PCR used 10 μM of the provided adaptor primer 1 and 10 μM of the gene specific primer (5′-RACE: CTGCATCACACAGGGTGTGCGGCCGT; 3′-RACE: CTGCTGCCC AGTGCCAACTCCTTCTGCTAT) in a 25 μl reaction containing 0.1 ng/μl of human testis or brain Marathon-Ready cDNA, followed by an inner PCR reaction with the nested adaptor primer 2 and the nested gene specific primer (5′-RACE: CTGCATCACACAGGGTGTGCGGCCGT; 3′-RACE: GTCCTGGAG CAGCGGCCCTACAGACGGGG). RACE was performed per Advantage-GC 2 PCR kit manufacturer standard protocol (BD Biosciences). PCR products were then subcloned into pCR2.1-TOPO vector for sequencing.

According to the cloned consensus RACE products, we designed new primers flanking *KCNJ18* (see Mutational Analysis, below). The PCR was performed in a 25 μl reaction with 5 μl of substrate (0.1 ng/μl of human testis Marathon-Ready cDNA) (Clontech, Palo Alto, CA) under the following touchdown PCR conditions: 5 min at 94°C, followed by 38 cycles of 20 s at 94°C, touchdown annealing temperature step of 30 s at 68°C /−0.5°C per cycle, and an extension step of 2 min at 72°C. This was repeated using skeletal muscle cDNA from FirstChoice RACE-Ready cDNA (Ambion, Austin, TX) to validate the full-length *KCNJ18* cDNA. Products were subcloned into pCR2.1-TOPO and sequenced.

Kir2.6 Multiple-Tissue Northern Blot Expression

Exon 1 of *KCNJ12* (primers: GAGATCAGATAACAGCCGGCGGG/CTTCTC TGCAAAGCGGATCG) and *KCNJ18* (primers: CTCTGTGGGACAGATACT GAAGCC/GACACGATGCTGTAGGGGTTG) were used as probes after random prime labeling with ^{32}P dCTP at 37°C for 4 hr with the Rediprime II Random Prime Labeling kit (Amersham Biosciences, Piscataway, NJ). Ready-to-use Multiple Tissue Northern membrane (Clontech, Palo Alto, CA) was then hybridized at 68°C in ExpressHyb Hybridization Solution (BD Biosciences, Palo Alto, CA) at a concentration of 1–2 × 10^6 cpm/ml (2–10 ng/ml). After overnight hybridization, the membrane was washed 2 × 20 min in 2× SSC/0.05% SDS at room temperature, followed by another two washes for 20 min each in 0.1× SSC/0.1% SDS at 55°C for *KCNJ18* and at room temperature for *KCNJ12*. The timing of washes was optimized according to radioactivity counting and the blot was exposed for 60 hr with Kodak x-OMAT AR film (Eastman Kodak, Rochester, NY) film and an intensifying screen.

Promoter Constructs

Inspection of the possible *KCNJ18* promoter sequence revealed a region containing a DR4 motif (5′-TGACCTggccTCACCTcaggg-3′), located 265 bp upstream of exon 1. We used the above TRE sequence as an oligonucleotide with an inner EcoRI restriction site combined with NheI linker in the forward strand (5′-CTAGCggaattccTGACCTGGCCTcACCTCAGGG-3′) and BglII linker in the reverse (5′-TCTAGCCCTGAGGTgAGGCCAGGTCAggaattcc). The NheI/BglII-linked TRE sequence was ligated into pGL3-Basic (Promega, Madison, WI) to produce the WT construct. Negative controls were made either by disruption of the TRE sequence (5′-CTAGCggaattccTGgaCTGΔCT cgaCTCAGGG-3′) (mutant construct) or by release of the NheI/BglII fragment and recircularization of the vector ("Empty" pGL3). A positive control was constructed with two TRE binding motifs (2xDR-4pGL3).

T3 Treatment and Luciferase Assay

Wild-type, mutant, and empty vectors were used for transient transfection of C2C12 or 293T cells. Transfections were carried out in duplicate using Lipofectamine 2000 (Invitrogen) according to the manufacturer's instructions. C2C12 cells (1.25 × 10 cells/well for "proliferating" and 3 × 10 cells/well for "differentiated" stage, which is believed to be more similar to native muscle, in 24-well plates) were seeded each day prior to transfection. The cells were transfected with 0.5 μg pGL3 construct, 0.1 μg internal control plasmid pRL-TK (Promega) that constitutively expresses renilla luciferase, and 0.5 μg expression plasmid for human thyroid receptor (TRβ). C2C12 cells were first cultured in Dulbecco's modified Eagle's medium (DMEM) with 10% fetal bovine serum (FBS) and 10% horse serum (HS), followed by 10% (proliferating) or 2% (differentiated) HS solely, containing penicillin and streptomycin (100 μg/ml). T3-depleted serum was obtained by AG1-X8 resin (BioRad) treatment for 16 hr at room temperature. The cells were harvested 48 (proliferating) or 72 (differentiated) hours posttransfection. Serum-free medium (DMEM) supplemented with 2 mg/ml of T3-free bovine serum albumin (Sigma) was used for transfection.

In both cell types, triiodothyronine (T3, Sigma) was added 6 hr after transfection to the labeled concentration. 293T cells were harvested 24 hr after transfection. Cellular expression of the luciferases was assayed using a dual luciferase assay system (Promega). Light intensity was measured with a TD-20/20 DLR luminometer (Turner BioSystems). The assay was replicated five times. Relative light unit measures were obtained in duplicate in each assay.

Mutational Analysis

The entire coding region (1.47 Kb) of *KCNJ18* was specifically amplified and sequenced in TPP patients and healthy controls. We performed PCR of *KCNJ18* (primers: ATGCTGTCCTCTCTGTTCC/GGGCCTCTCCCCGGCCA)

using 20–100 ng genomic DNA in a 25 μl reaction using the Advantage 2 polymerase mix (Clontech) with the addition of 5 μl GC-melt from the Advantage-GC 2 polymerase mix. Cycling conditions were as follows: 95°C for 1 min followed by 35 cycles of 94°C for 30 s and 67°C for 3 min, plus a final 3 min extension at 67°C. All sequences were collected and analyzed with Sequencher (Gene Code Corporation, Ann Arbor, MI) software. Sequencing was performed twice in both directions for each sample. Uniqueness of *KCNJ18* sequencing was confirmed by the lack of polymorphisms at amino acids 15 and 430, at which *KCNJ18* and *KCNJ12* differ (Table S2).

Electrophysiology

293T cells were maintained as described above and transfected with 2 μg DNA using Polyfect (QIAGEN, Valencia CA). Currents were recorded 24–72 hr after transfection.

All recordings were conducted at room temperature with an Axopatch 200B Amplifier (Axon Instruments, Union City, CA) and pClamp6 for data acquisition. Data were analyzed with Igor Pro (Wavemetrics, Oswego, OR) and QUB (http://www.qub.buffalo.edu/). Pippettes (Kimax) of 1.5–3.5 MΩ were coated with Sylgard 184 (Dow Corning Corporation, Midland, MI) and heat polished prior to use. Series resistance and capacitance compensation of 95% was used for all whole-cell recordings. For whole-cell recordings, each trial consisted of maintaining cells at resting membrane potential for 50 ms, a 100 ms test pulse between −60 mV to +60 mV in 10 mV increments, and then returning cells to resting membrane potential. Five trials were run per cell and used to create a per-cell average. Data was sampled at 5 kHz with a 2 kHz low-pass filter. Intracellular solution was as follows: 110 mM K-Aspartate, 20 mM KCl, 1 mM $MgCl_2$, 10 mM EGTA, 5 mM Na_2-ATP, 5 mM glucose, and 10 mM HEPES (pH 7.4). Cells were bathed in a solution of 117 mM NaCl, 30 mM KCl, 2 mM $CaCl_2$, 1 mM $MgCl_2$, 10 mM HEPES, 5 mM glucose, and 2 mM $NaHCO_3$ (pH 7.3) or the equivalent solution with TEA-Cl substituted for KCl to measure leak.

Single-channel on-cell and multichannel inside-out excised patch currents were recorded at 50 kHz continuously for 1–7 min at the test voltage with a 1 kHz low-pass filter. For single-channel recordings, pipette and bath solution was comprised of 150 mM KCl, 2 mM $MgCl_2$, 1 mM EGTA, and 10 mM HEPES (pH 7.4). This solution was also used as the bath solution for excised patches while the pipette solution was identical to bath solution used for whole-cell recordings. Excised patches were held at −80 mV during recordings. Where indicated, 100 nM PMA or 300 μg/ml polylysine (Sigma) was added. Cells were bathed in PMA at least 45 min prior to recording. After idealization, data for excised inside-out patches was summed and fit with an exponential function: base + A*exp($-x/T_{50}$). Similar results can be obtained by instead fitting with a Hill or Boltzmann-style sigmoid function. Single-channel current levels were calculated by curve fitting the sum of a number of Gaussian curves to the recorded data. Open probability was then calculated as the relative areas of these Gaussian curves. For the T354E and WT + PMA recordings, single-channel conductance was calculated at −60 mV only, as other potentials lacked sufficient openings for reliable measurement. Data are reported as mean ± standard error (n = number of cells, patches, etc.) unless otherwise noted. For all figures, * denotes $p < 0.05$, ** $p < 0.01$, and *** $p < 0.001$.

ACCESSION NUMBERS

The sequence of KCNJ18 reported in this paper has been deposited in the NCBI database under accession number FJ434338.

SUPPLEMENTAL INFORMATION

Supplemental Information includes four figures and five tables and can be found with this article online at doi:10.1016/j.cell.2009.12.024.

ACKNOWLEDGMENTS

We thank Lily Jan, Friederike Haas, and Carol Vandenburg for helpful discussions and advice and all the patients for their participation. We also thank Kathleen Giacomini for additional DNA controls. This work was supported by the Muscular Dystrophy Association, National Institutes of Health grant U54 RR19481, CAPES Foundation grant 2284/01-4 (MRDS), and FAPESP (Sao Paulo State Research Foundation) grants 2000/03442-4 (MRDS) and 1999/03688-4 (RMBM). B.F. is supported by INSERM, AFM, and ANR Maladies Rares and acknowledges patient referral and fruitful discussions of members of the clinical and research French network Résocanaux. R. Brown received generous support from the C.B. Day Foundation and the NINDS L.J.P. is an Investigator of the Howard Hughes Medical Institute.

Received: March 30, 2009
Revised: July 29, 2009
Accepted: December 4, 2009
Published: January 7, 2010

REFERENCES

Abraham, M.R., Jahangir, A., Alekseev, A.E., and Terzic, A. (1999). Channelopathies of inwardly rectifying potassium channels. FASEB J. *13*, 1901–1910.

Bailey, J.A., Yavor, A.M., Massa, H.F., Trask, B.J., and Eichler, E.E. (2001). Segmental duplications: organization and impact within the current human genome project assembly. Genome Res. *11*, 1005–1017.

Bassett, J.H., Harvey, C.B., and Williams, G.R. (2003). Mechanisms of thyroid hormone receptor-specific nuclear and extra nuclear actions. Mol. Cell. Endocrinol. *213*, 1–11.

Bulman, D.E., Scoggan, K.A., van Oene, M.D., Nicolle, M.W., Hahn, A.F., Tollar, L.L., and Ebers, G.C. (1999). A novel sodium channel mutation in a family with hypokalemic periodic paralysis. Neurology *53*, 1932–1936.

Donaldson, M.R., Jensen, J.L., Tristani-Firouzi, M., Tawil, R., Bendahhou, S., Suarez, W.A., Cobo, A.M., Poza, J.J., Behr, E., Wagstaff, J., et al. (2003). PIP2 binding residues of Kir2.1 are common targets of mutations causing Andersen syndrome. Neurology *60*, 1811–1816.

Eichler, E.E., Clark, R.A., and She, X. (2004). An assessment of the sequence gaps: unfinished business in a finished human genome. Nat. Rev. Genet. *5*, 345–354.

Hugnot, J.P., Pedeutour, F., Le Calvez, C., Grosgeorge, J., Passage, E., Fontes, M., and Lazdunski, M. (1997). The human inward rectifying K+ channel Kir 2.2 (KCNJ12) gene: gene structure, assignment to chromosome 17p11.1, and identification of a simple tandem repeat polymorphism. Genomics *39*, 113–116.

Karle, C.A., Zitron, E., Zhang, W., Wendt-Nordahl, G., Kathöfer, S., Thomas, D., Gut, B., Scholz, E., Vahl, C.F., Katus, H.A., and Kiehn, J. (2002). Human cardiac inwardly-rectifying K+ channel Kir(2.1b) is inhibited by direct protein kinase C-dependent regulation in human isolated cardiomyocytes and in an expression system. Circulation *106*, 1493–1499.

Kavok, N.S., Krasilnikova, O.A., and Babenko, N.A. (2001). Thyroxine signal transduction in liver cells involves phospholipase C and phospholipase D activation. Genomic independent action of thyroid hormone. BMC Cell Biol. *2*, 5.

Kelley, D.E., Gharib, H., Kennedy, F.P., Duda, R.J., Jr., and McManis, P.G. (1989). Thyrotoxic periodic paralysis. Report of 10 cases and review of electromyographic findings. Arch. Intern. Med. *149*, 2597–2600.

Krapivinsky, G., Medina, I., Eng, L., Krapivinsky, L., Yang, Y., and Clapham, D.E. (1998). A novel inward rectifier K+ channel with unique pore properties. Neuron *20*, 995–1005.

Kung, A.W. (2002). Thyrotoxic Periodic Paralysis. In Oxford Textbook of Endocrinology and Diabetes, J.A.H. Wass, S.M. Shalet, and E.A.M. Gale, eds. (Oxford: Oxford University Press), pp. 427–429.

Kung, A.W. (2006). Clinical review: thyrotoxic periodic paralysis: a diagnostic challenge. J. Clin. Endocrinol. Metab. *91*, 2490–2495.

Le Bouter, S., Demolombe, S., Chambellan, A., Bellocq, C., Aimond, F., Toumaniantz, G., Lande, G., Siavoshian, S., Baró, I., Pond, A.L., et al. (2003). Microarray analysis reveals complex remodeling of cardiac ion channel expression with altered thyroid status: relation to cellular and integrated electrophysiology. Circ. Res. *92*, 234–242.

Leonoudakis, D., Conti, L.R., Anderson, S., Radeke, C.M., McGuire, L.M., Adams, M.E., Froehner, S.C., Yates, J.R., 3rd, and Vandenberg, C.A. (2004a). Protein trafficking and anchoring complexes revealed by proteomic analysis of inward rectifier potassium channel (Kir2.x)-associated proteins. J. Biol. Chem. *279*, 22331–22346.

Leonoudakis, D., Conti, L.R., Radeke, C.M., McGuire, L.M., and Vandenberg, C.A. (2004b). A multiprotein trafficking complex composed of SAP97, CASK, Veli, and Mint1 is associated with inward rectifier Kir2 potassium channels. J. Biol. Chem. *279*, 19051–19063.

Lin, H.Y., Davis, F.B., Gordinier, J.K., Martino, L.J., and Davis, P.J. (1999). Thyroid hormone induces activation of mitogen-activated protein kinase in cultured cells. Am. J. Physiol. *276*, C1014–C1024.

Lopes, C.M., Zhang, H., Rohacs, T., Jin, T., Yang, J., and Logothetis, D.E. (2002). Alterations in conserved Kir channel-PIP2 interactions underlie channelopathies. Neuron *34*, 933–944.

Lu, Z. (2004). Mechanism of rectification in inward-rectifier K+ channels. Annu. Rev. Physiol. *66*, 103–129.

Namba, N., Inagaki, N., Gonoi, T., Seino, Y., and Seino, S. (1996). Kir2.2v: a possible negative regulator of the inwardly rectifying K+ channel Kir2.2. FEBS Lett. *386*, 211–214.

Namba, N., Mori, R., Tanaka, H., Kondo, I., Narahara, K., and Seino, Y. (1997). The inwardly rectifying potassium channel subunit Kir2.2v (KCNJN1) maps to 17p11.2—>p11.1. Cytogenet. Cell Genet. *79*, 85–87.

Nemzek, J.A., Kruger, J.M., Walshaw, R., and Hauptman, J.G. (1994). Acute onset of hypokalemia and muscular weakness in four hyperthyroid cats. J. Am. Vet. Med. Assoc. *205*, 65–68.

Nichols, C.G., and Lopatin, A.N. (1997). Inward rectifier potassium channels. Annu. Rev. Physiol. *59*, 171–191.

Plaster, N.M., Tawil, R., Tristani-Firouzi, M., Canún, S., Bendahhou, S., Tsunoda, A., Donaldson, M.R., Iannaccone, S.T., Brunt, E., Barohn, R., et al. (2001). Mutations in Kir2.1 cause the developmental and episodic electrical phenotypes of Andersen's syndrome. Cell *105*, 511–519.

Preisig-Müller, R., Schlichthörl, G., Goerge, T., Heinen, S., Brüggemann, A., Rajan, S., Derst, C., Veh, R.W., and Daut, J. (2002). Heteromerization of Kir2.x potassium channels contributes to the phenotype of Andersen's syndrome. Proc. Natl. Acad. Sci. USA *99*, 7774–7779.

Ptácek, L.J., Tawil, R., Griggs, R.C., Engel, A.G., Layzer, R.B., Kwieciński, H., McManis, P.G., Santiago, L., Moore, M., Fouad, G., et al. (1994). Dihydropyridine receptor mutations cause hypokalemic periodic paralysis. Cell *77*, 863–868.

Ryan, D.P., and Ptácek, L.J. (2007). Ion channel disorders. In The Molecular and Genetic Basis of Neurologic and Psychiatric Disease, R.N. Rosenberg, S. DiMauro, H.L. Paulson, L.J. Ptácek, and E.J. Nestler, eds. (Philadelphia: Lippincott Williams & Wilkins), pp. 550–568.

Silva, M.R., Chiamolera, M.I., Kasamatsu, T.S., Cerutti, J.M., and Maciel, R.M. (2004). Thyrotoxic hypokalemic periodic paralysis, an endocrine emergency: clinical and genetic features in 25 patients. Arq. Bras. Endocrinol. Metabol. *48*, 196–215.

Soom, M., Schönherr, R., Kubo, Y., Kirsch, C., Klinger, R., and Heinemann, S.H. (2001). Multiple PIP2 binding sites in Kir2.1 inwardly rectifying potassium channels. FEBS Lett. *490*, 49–53.

Takahashi, N., Morishige, K., Jahangir, A., Yamada, M., Findlay, I., Koyama, H., and Kurachi, Y. (1994). Molecular cloning and functional expression of cDNA encoding a second class of inward rectifier potassium channels in the mouse brain. J. Biol. Chem. *269*, 23274–23279.

Tinker, A., Jan, Y.N., and Jan, L.Y. (1996). Regions responsible for the assembly of inwardly rectifying potassium channels. Cell *87*, 857–868.

Wible, B.A., De Biasi, M., Majumder, K., Taglialatela, M., and Brown, A.M. (1995). Cloning and functional expression of an inwardly rectifying K+ channel from human atrium. Circ. Res. *76*, 343–350.

Zaritsky, J.J., Eckman, D.M., Wellman, G.C., Nelson, M.T., and Schwarz, T.L. (2000). Targeted disruption of Kir2.1 and Kir2.2 genes reveals the essential role of the inwardly rectifying K(+) current in K(+)-mediated vasodilation. Circ. Res. *87*, 160–166.

Zaritsky, J.J., Redell, J.B., Tempel, B.L., and Schwarz, T.L. (2001). The consequences of disrupting cardiac inwardly rectifying K(+) current (I(K1)) as revealed by the targeted deletion of the murine Kir2.1 and Kir2.2 genes. J. Physiol. *533*, 697–710.

Zobel, C., Cho, H.C., Nguyen, T.T., Pekhletski, R., Diaz, R.J., Wilson, G.J., and Backx, P.H. (2003). Molecular dissection of the inward rectifier potassium current (IK1) in rabbit cardiomyocytes: evidence for heteromeric co-assembly of Kir2.1 and Kir2.2. J. Physiol. *550*, 365–372.

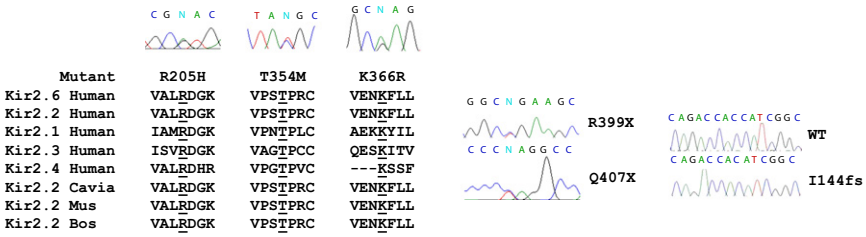

Figure S1. Kir 2.6 Mutations Found in Our TPP Cohort and Their Conservation across Species—Related to Figure 1

A total of six mutations were found in our cohort of TPP patients. Chromatograms from mutations with R205H, T354M, K366R, R399X, Q407X, and I144fs (versus wild-type) are shown. The missense mutations (R205H, T354M, and K366R) are at residues that are well conserved both among human Kir2 family members as well as across other species (position of the mutation is underlined).

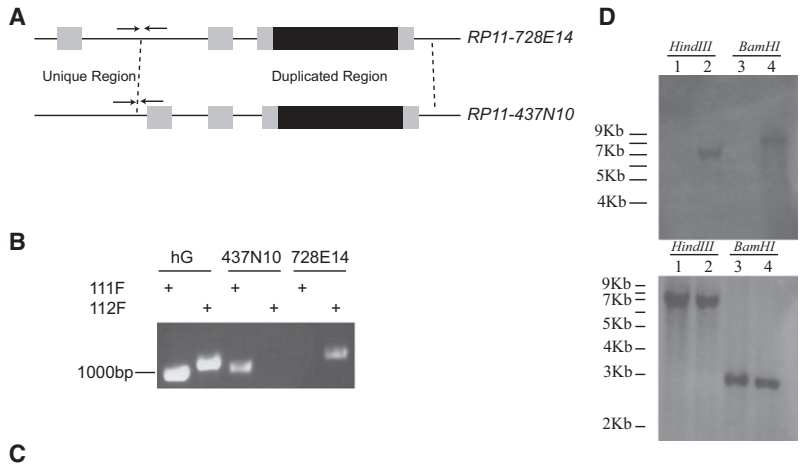

C

```
111_Genomic AGANGGATCTCCAGGAAGTGTCTCCCTGACNGACTGGGAAGTCATCTTTATTGAAGACATTTGGCCAGAGNGAGAGGCAT
112_Genomic TCACAGCACCAATTAGCTGCCACCAAAGGAATGGGAGAGAGGCAGGCAAGAGCCACATAGTCAGGGAAGGCTTCCTGGAG
RP11-437N10 AGACGGATCTCCAGGAAGTGTCTCCCTGACGGACTGGGAAGTCATCTTTATTGAAGACATTTGGCCAGAGTGAGAGGCAT
RP11-728E14 TCACAGCACCAATTAGCTGCCACCAAAGGAATGGGAGAGAGGCAGGCAAGAGCCACATAGTCAGGGAAGGCTTCCTGGAG
Cons          *: *  *                *   *        *  ** **          * * * *  *  *  *  *   * *

111_Genomic CCAGGCCCCTGAGAAACAGGGGAGGCAGAGCAAGAGGGAGGACAGAGCAGAGGCCAGAGCCCANGCAGGATACAGCATCG
112_Genomic GAGGTGGTCCAAGCCAGACTTGGAGTGACTGTGGTGTCTCCTAGAGACACCAGGGCCAACGTGCGTGGTCAAATCCTAGG
RP11-437N10 CCAGGCCCCTGAGAAACAGGGGAGGCAGAGCAAGAGGGAGGACAGAGCAGAGGCCAGAGCCCACGCAGGATACAGCATCG
RP11-728E14 GAGGTGGTCCAAGCCAGACTTGGAGTGACTGTGGTGTCTCCTAGAGACACCAGGGCCAACGTGCGTGGTCAAATCCTAGG
Cons            *    *  **  * *   *  *        * *           **   *    * *   :   *   *   *   *
                                  Unique ←┬→ Duplicated
111_Genomic TGCCACTGCCACNGGCATAAGGGGCGGTGAATTTCTATCCCAGCTTTGCCATGGACTGGCTGCNTTTCCCTAGGCACGGC
112_Genomic TCTCTATTTCCACAGCCCTGGAAGTCCTGAATTTCTATCCCAGCTTTGCCATGGACTGGCTGCGTGTCCCTAGGCACAGC
RP11-437N10 TGCCACTGCCACAGGCATAAGGGGCGGTGAATTTCTATCCCAGCTTTGCCATGGACTGGCTGCATTTCCCTAGGCACGGC
RP11-728E14 TCTCTATTTCCACAGCCCTGGAAGTCCTGAATTTCTATCCCAGCTTTGCCATGGACTGGCTGCGTGTCCCTAGGCACAGC
Cons        *     *  *    **    *  *   ************************************:* *********** **

111_Genomic ACTCATCCTAACTGATCCCCAGTTTCTTGCCTCTATCAAAAGAAACTAATGTGAATGGAAATGGCATGTGTCACAGTGAT
112_Genomic ACTCATCCTATCCGAGCCCCAGTTTCTTGCCTCTATCAAAAGAAACTGGTGTGAATGGAAGTGGCATGTGTCACAGTGAC
RP11-437N10 ACTCATCCTAACTGATCCCCAGTTTCTTGCCTCTATCAAAAGAAACTAATGTGAATGGAAATGGCATGTGTCACAGTGAT
RP11-728E14 ACTCATCCTATCCGAGCCCCAGTTTCTTGCCTCTATCAAAAGAAACTGGTGTGAATGGAAGTGGCATGTGTCACAGTGAC
Cons        ********** * ** ******************************  *********** ******************

111_Genomic GAGTGTTCCTGATGCACAGCAGTTGCGCACTTCCAGTTTACTGGGGTTGGAAAGCGTGTGTGGCAGTAAGAGGTCCGTGC
112_Genomic GAGTGTTCCTGACGCACAGCAGTTGCGCAGTCCCAGTTTACTGGGGTTGGAAAGCGTGTGTGGCAGTAAGAGGTCCGTGC
RP11-437N10 GAGTGTTCCTGATGCACAGCAGTTGCGCACTTCCAGTTTACTGGGGTTGGAAAGCGTGTGTGGCAGTAAGAGGTCCGTGC
RP11-728E14 GAGTGTTCCTGACGCACAGCAGTTGCGCAGTCCCAGTTTACTGGGGTTGGAAAGCGTGTGTGGCAGTAAGAGGTCCGTGC
Cons        ************ ***************** * ************************************************

111_Genomic AAGGNGGTATGGGGTCAGAACAGCCTCTGTGGGGCCCCGCTCGCNACCNTCTAGCTATGGAGAGCCTGAGTCTCCTCACT
112_Genomic AAAGCGGTATGGGGTCAGAACAGCCTCTGTGGGGCCCCGCTCGCTACCGTCTAGCTGTGGGGTGCCTGAGTCTCCTCACT
RP11-437N10 AAGGCGGTATGGGGTCAGAACAGCCTCTGTGGGGCCCCGCTCGCTACCGTCTAGCTATGGAGAGCCTGAGTCTCCTCACT
RP11-728E14 AAAGCGGTATGGGGTCAGAACAGCCTCTGTGGGGCCCCGCTCGCTACCGTCTAGCTGTGGGGTGCCTGAGTCTCCTCACT
Cons        ** *:*************************************:***:******* *** * *****************
```

Figure S2. *KCNJ18* and *KCNJ12* Are Unique—Related to Figure 2

Alignment of the BACs containing *KCNJ12* (RP11-728E14) and *KCNJ18* (RP11-437N10) suggests that *KCNJ18* is largely a duplication of *KCNJ12* (A, diagram as in Figure 1 where dashed lines indicate duplication boundaries and arrows primer position). The duplication/unique region boundary can be specifically amplified from each BAC using a specific forward primer (111F: CCCAATCAAGCAGAAACACA or 112F: CCTGCTAGATCCCAGCTCAG) and a non-specific reverse primer (111R; GGAGAAACCGGAGAAACACA), indicating that the BACs are unique (B). Both primer pairs are also able to produce different PCR products from human genomic DNA (hG). Alignment of the sequence of both BAC and human genomic PCR products indicates that the amplicons from an individual primer pair match between BAC and human genomic DNA, but not between primer pairs except in the duplicated region (C). A portion of the sequence is shown for both genomic DNA (111_Genomic or 112_Genomic for amplicon from 111F or 112F primer, respectively) and BAC DNA is shown. N indicates the presence of a polymorphism. Cons shows the conservation between all four sequences with a "*" indicating 100% conservation and a ":" indicating at least partial conservation, due to a polymorphism. The boundary of the unique and duplicated region is indicated. PCR from genomic DNA was performed with the same method used to screen for TPP mutations. BAC PCR was performed using Phusion DNA polymerase (Finnzymes, MA) according to the manufacturers instructions. Digested BAC DNA was probed with biotinylated synthetic probe targeted against either the unique exon 1 (CTGTTGGGAAGCCTGTTTC/ GTCACGAGGGTAAGCCAAGC, D top) or the conserved exon 3 (CAACCCCTACAGCATCGTGTC/TCCACACAGGTGGTGAACAT, D bottom). Both BACs were digested with BamHI or HindIII for 16 hr prior to fractionation. BAC RP11-728E14 was (digested as indicated) was run on lanes 1 and 3 while BAC Rp11-437N10 was run on lanes 2 and 4. Blots were performed simultaneously from the same digested DNA and gel. Expected sizes, according to reference BAC sequence, were: 0bp, D top 1; 7174bp, D top 2; 0bp, D top 3; 8408bp, D top 4; 6589bp, D bottom 1; 6572bp, D bottom 2; 2583bp, D bottom 3; 2583bp, D bottom 4.

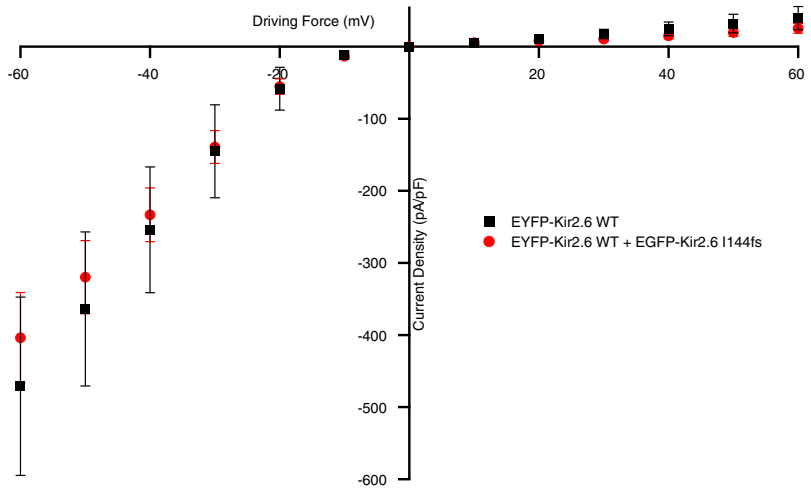

Figure S3. The I144fs Mutation Does Not Act in a Dominant Negative Manner—Related to Figure 4

Wild-type (black squares) channels were expressed in HEK293 cells at half their normal levels with or without an equivalent amount of I144fs mutant (red circles for WT + I144fs). Voltage steps indicate that the wild-type current is unaffected by coexpression of the I144fs (wild-type = −471.074 ± 123.65pA/pF and cotransfected = −402.898 ± 62.69pA/pF at −60mV).

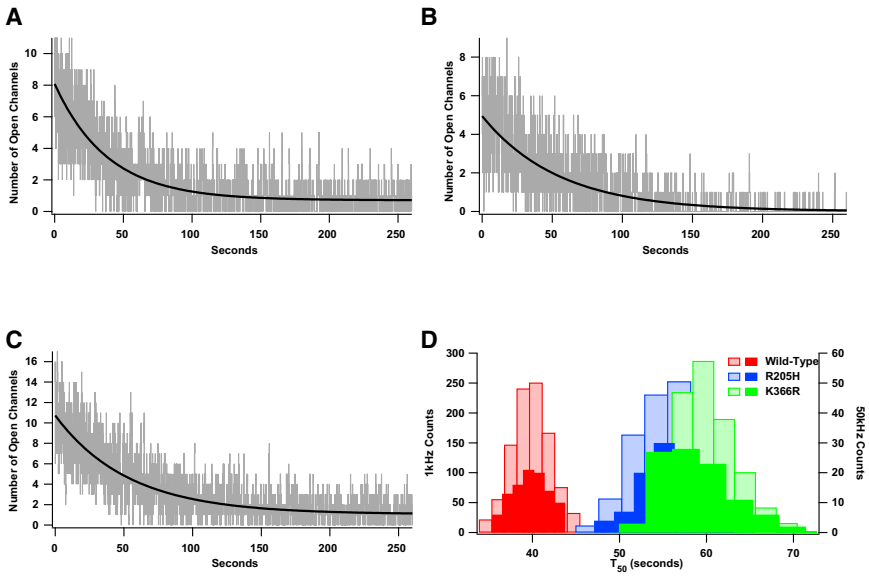

Figure S4. Statistical Modeling of Ion Channel PIP2 Interactions Indicates Robustness of T_{50} Estimations—Related to Figure 6

Individual idealized ion channel open and closed states were simulated in accordance to fit parameters from Figure 6. Open state dwell times were randomly selected from an exponential distribution with mean 220ms. Closed state dwell times were randomly selected from a similar distribution whose mean was altered over time such that the mean open probability would follow the curve fit from Figure 6. Initial open probability for each channel type was also taken from Figure 6 (0.65 for wild-type, 0.55 for R205H mutant, or 0.49 for K366R mutant). For each run, 11 (wild-type, A), 9 (R205H mutant, B) or 19 (K366R mutant, C), idealized openings were summed and fit with an exponential function as in Figure 6. Simulations were sampled at either 1kHz or 50kHz and the values derived from their fit stored and displayed as a histogram (D, light bars are 1kHz simulations and dark bars are 50kHz simulations). 1000 (1kHz sampling) or 100 (50kHz sampling) runs of each simulation were performed for each channel. The resulting T_{50} values have means 39.82 ± 0.07 s or 39.65 ± 0.20 s (Wild-type sampling 1kHz or 50kHz, respectively), 55.96 ± 0.13 s or 55.58 ± 0.34 s (R205H mutant 1kHz or 50kHz sampling, respectively), and 59.67 ± 0.11 s or 58.63 ± 0.40 s (K366R mutant 1kHz or 50kHz sampling, respectively). Simulations were run in Igor Pro (Wavemetrics). Similar results are seen if dwell times are chosen from Gaussian or gamma distributions (not shown).